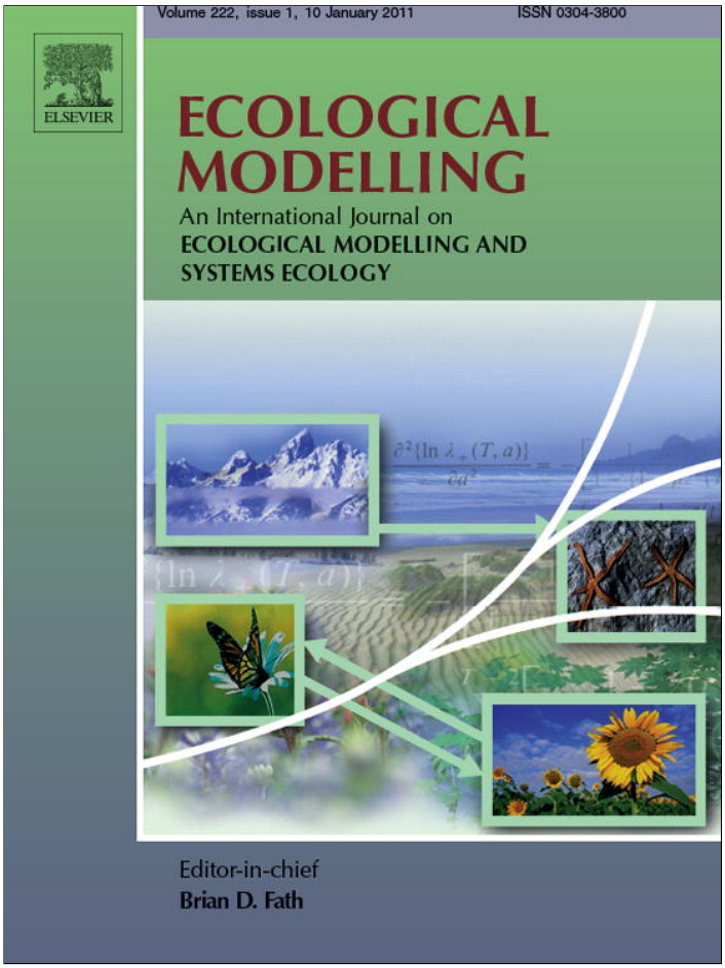

(This is a sample cover image for this issue. The actual cover is not yet available at this time.)

Ecological Modelling 222 (2011) 3568–3576

Contents lists available at SciVerse ScienceDirect

Ecological Modelling

journal homepage: www.elsevier.com/locate/ecolmodel

Predicting intertidal organism temperatures with modified land surface models

David S. Wethey*, Lindsay D. Brin[1], Brian Helmuth, K.A.S. Mislan[2]

Department of Biological Sciences, University of South Carolina, 715 Sumter Street, Columbia, SC 29208, United States

ARTICLE INFO

Article history:
Received 21 February 2011
Received in revised form 19 August 2011
Accepted 22 August 2011

Keywords:
Temperature
Intertidal
Mussel
Biophysics
Meteorology
Forecasting

ABSTRACT

Animals and plants in the marine intertidal zone live at the interface between terrestrial and marine environments. This zone is likely to be a sensitive indicator of the effects of climate change in coastal ecosystems, because of several key characteristics including steep environmental gradients, rapid temperature changes during tide transitions, fierce competition for limited space, and a community of mostly sessile organisms. Here we describe a modular modeling approach using modifications to a meteorological land surface model to determine body temperatures of the ecologically dominant rocky intertidal mussel *Mytilus californianus*, as a tool that can be used as a proxy for ecological performance. We validate model results against *in situ* measurements made with biomimetic body temperature sensors. Model predictions lie within the range of variability of biomimetic measurements, based on observations over a 4-year period at sites along 1700 km of the US west coast from southern California (34.5°N) to northern Washington (48.4°N). Our modular approach can be easily applied to many situations in the intertidal zone, including bare rock, mussel, barnacle, and algal beds, salt-marsh grasses, and sand- and mud-flats, by modifying the "vegetation layer" in a standard meteorological land surface model. Biophysical models such as these, which link ecological processes to changing climates through predictions of body temperature, are essential for understanding biogeographic patterns of physiological stress and mortality risk.

1. Introduction

To predict ecological and biodiversity responses to climate change, it is essential to integrate ecological processes into climate models. Here we show how coupled biological and climate models can be used to explore ecological questions in the marine intertidal zone, which has long served as a model system for studying the interactive effects of physical and biotic processes on patterns of abundance, biodiversity and ecosystem function (e.g. Connell, 1961; Lewis, 1964; Paine, 1966).

The marine intertidal ecosystem, situated at the interface between the land and ocean, has steep environmental gradients in climate variables that resemble altitudinal gradients in the terrestrial environment, but which occur on the scale of <10 m. Environmental gradients in the marine intertidal zone are determined by the duration and timing of exposure to atmospheric conditions, which are controlled by the movement of the tides. During low tide (atmospheric conditions), marine intertidal organisms experience extremes in body temperature, which can be important determinants of local and geographic distribution patterns (e.g. Southward, 1958; Wethey, 2002; Wethey et al., 2011; Williams et al., 2005). Due to the steepness of the desiccation and temperature gradients, intertidal organisms often live close to their physiological limits (e.g. Foster, 1969, 1971; Jones et al., 2009, 2010; Wolcott, 1973) and are likely to be sensitive to relatively minor changes in terrestrial climate (Gilman et al., 2006; Somero, 2002).

The regional climate projections in the Fourth Assessment Report by the Intergovernmental Panel on Climate Change show that in Western North America, a region that supports a diversity of intertidal organisms (Morris et al., 1980), there will 'very likely' be more frequent heat waves with longer duration and greater intensity by the end of the 21st century, a finding that was consistent across 21 Atmosphere-Ocean General Circulation Models (Beniston et al., 2007; Christensen et al., 2007). As a result, predicting patterns of aerial body temperature in coastal ecosystems is of pressing concern if we are to predict how changes in terrestrial climate are likely to affect this ecosystem.

Historically, heat and mass budget models of individual organisms have been the standard for modeling organism temperatures (e.g. Bell, 1995; Buckley, 2008; Gates, 1980; Helmuth, 1998; Kearney and Porter, 2004; Miller et al., 2009; Tracy, 1976). These

* Corresponding author. Tel.: +1 803 777 3936; fax: +1 803 777 4002.
E-mail addresses: wethey@biol.sc.edu (D.S. Wethey), lindsay.brin@gmail.com (L.D. Brin), helmuth@environ.sc.edu (B. Helmuth), kas.mislan@gmail.com (K.A.S. Mislan).
[1] Present address: Department of Ecology and Evolutionary Biology, Brown University, 80 Waterman Street, Box G-W, Providence, RI 02912, United States.
[2] Present address: Program in Atmospheric and Oceanic Sciences, Princeton University, 300 Forrestal Road, Sayre Hall, Princeton, NJ 08544, United States.

0304-3800/$ – see front matter © 2011 Elsevier B.V. All rights reserved.
doi:10.1016/j.ecolmodel.2011.08.019

one-of-a-kind models have been very successful in linking meteorological conditions to body temperatures of organisms in both terrestrial and aquatic environments. These studies demonstrated that there are strong effects of body temperatures on local distribution (Bell, 1995; Miller et al., 2009), biogeography (Buckley, 2008; Kearney and Porter, 2004), and ecological performance (Gates, 1980; Tracy, 1976). In the intertidal zone, previous workers have used biophysical methods to develop one-of-a-kind models for intertidal mussels (Helmuth, 1998; Gilman et al., 2006; Finke et al., 2009), barnacles (Wethey, 2002), starfish (Szathmary et al., 2009), limpets (Miller et al., 2009), and algae (Bell, 1995). These models have confirmed the view that the intertidal zone has an extraordinary daily temperature range, and that intertidal organisms are generally living close to their physiological limits. Despite their successes, these models are not transferable to other species or habitats without considerable programming effort. They were written for specific organisms and environments, and cannot be easily modified to model different organisms in different habitats. This paper describes the first attempt to build a generic intertidal model that can easily be converted from one type of organism to another as is routinely done in meteorological land surface models.

Here we describe a modular approach to modeling organismal temperatures, based on modifications to the "vegetation layer" of a meteorological land surface model, which is used operationally for the US National Weather Service forecasts (Ek et al., 2003). We used this modular model to determine the body temperature of rocky intertidal mussels in the genus *Mytilus*. We focused on this ecological dominant because, like the trees of terrestrial forests, *Mytilus* mussel species control the dynamics of the rest of the community (e.g. Paine, 1966, 1974). Permanent residents of the intertidal ecosystem, including mussels, are ectotherms, meaning that body temperature is determined by heat exchange with the external environment. Because of this, there is a tight link between body temperature and ecology. Survival rates, metabolic rates, and demographic rates are all strongly influenced by body temperature (Bayne et al., 1976; Bayne and Worrall, 1980; Jones et al., 2009, 2010; Widdows and Bayne, 1971). Therefore, body temperature can serve as a proxy for ecological performance.

By modifying the operational model, we took advantage of decades of sophisticated modeling and validation (e.g. Ek et al., 2003), and, by making minor changes to the original software, we applied the underlying physical processes to an ecologically sensitive habitat. We used weather station data or outputs of standard weather and climate simulations as forcing variables, with the addition of data on ocean immersion times (because of the tide) and sea surface temperature. We validated model results against *in situ* temperature measurements made using biomimetic sensors that mimic the thermal characteristics of living mussels. We also compared results against an earlier one-of-a kind heat budget model that we developed *de novo* to estimate the body temperatures of mussels (Gilman et al., 2006).

We carried out this analysis as a demonstration that biologically relevant temperature models for many situations in the intertidal zone, including bare rock surfaces, mussel beds, barnacle beds, algal beds, salt-marsh grass beds, sandflats, and mudflats, can be rapidly developed from standard meteorological land surface models by creating new "vegetation types" with appropriate physical properties.

2. Model development

2.1. Organisms

The model organism chosen for this analysis was the marine mussel *Mytilus californianus*, a marine bivalve mollusk that attaches to intertidal rock surfaces with byssus threads. The shells

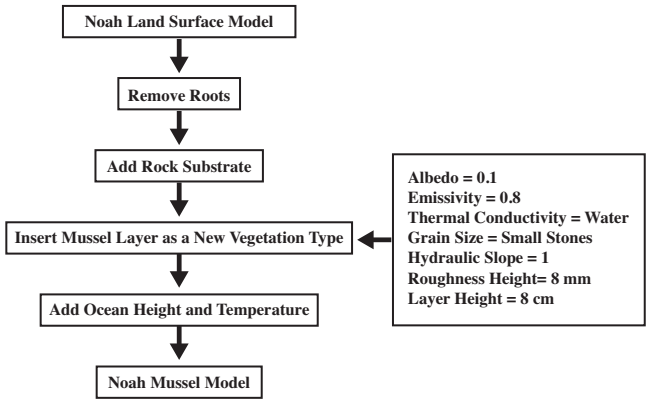

Fig. 1. Conceptual diagram showing the modifications made to the NOAH Land Surface model for ecological studies of marine intertidal mussel species.

are typically black, although when eroded, they become lighter in color. These animals are sedentary and form extensive aggregations or beds that cover much of the intertidal surface, and they competitively exclude most other sessile species (Paine, 1974). *M. californianus* has an upper thermal limit of approximately 38 °C (Denny et al., 2011), and experiences heat stress at 30 °C, as indicated by expression of heat shock proteins (Helmuth and Hofmann, 2001). At 26 °C it suffers a metabolic deficit during low tide (Bayne et al., 1976). Its body temperature at high tide is equal to sea surface temperature, and at low tide its body temperature exceeds air temperature often by 10 °C or more (Helmuth and Hofmann, 2001).

2.2. General model structure

We based our intertidal model on the NOAH land surface model (NOAH LSM) (Chen and Dudhia, 2001; Ek et al., 2003), a 1-dimensional model which includes radiative exchanges between the sky and ground, as well as convective, evaporative, and conductive heat exchange, and hydrology, and is used as the land component of atmospheric models and reanalysis products by the US National Weather Service (Ek et al., 2003; Mesinger et al., 2006; Saha et al., 2010). The NOAH LSM includes a vegetation layer that determines evapotranspiration rates, as well as heat transfer between the atmosphere and the land surface.

2.3. NOAH Mussel Model

In constructing the NOAH Mussel Model, we modified the NOAH LSM in several minor ways. In order to simulate temperatures of intertidal mussel beds, we created a new "vegetation type" with the heat and mass transfer characteristics of mussels (measured by Helmuth, 1998), and an underlying solid rock substratum (Fig. 1). Since intertidal animals do not carry out evapotranspiration, nor do they have roots for water transport, these characteristics were removed from the new "vegetation type". It was necessary to allow periodic flooding of the surface by the rising and falling tide and by wave splash, so sea surface temperature was added as input to the model along with an indicator to distinguish the times when the surface was exposed to atmospheric conditions or submerged. All of the physics in the NOAH LSM were left intact; only these physical properties of the intertidal mussel bed on rock were introduced (a conceptual diagram of the process is shown in Fig. 1, and a summary of differences among the models is in Table 1):

(1) For rocky intertidal surfaces, the porous soil layers were replaced with impermeable granite layers (Table 1).
(2) The top soil layers were replaced with layers that had the heat transfer characteristics of mussels, including a black color (an

Table 1
Summary of differences among models.

	NOAH Mussel (this paper)	NOAH LSM (Ek et al., 2003)	Gilman et al. (2006)
Vegetation	Mussel bed	Bare soil	Mussel bed
Roots	None	None	None
Albedo	0.1	0.1	0.1
Longwave emissivity	0.8	1.0	0.75
Roughness height	0.008	0.011	0.008
Vegetation thermal conductivity	Water	Soil	Water
Vegetation specific heat	Water	Soil	Water
Soil type	Stone	Soil	Stone
Submergence by tide	Yes	No	Yes
Water drainage	Hydraulic slope	Hydraulic slope	Instantaneous
Surface evaporation	Nonlinear	Nonlinear	Linear
Passive convection	Yes	Yes	No
Number of layers	20	20	50
Depth of bottom layer	133 cm	133 cm	50 cm

albedo of 0.1), a long-wave emissivity of 0.80, specific heat and thermal conductivity equivalent to water, a grain size equivalent to small stones, a hydraulic slope of 1.0, and a roughness height of 8 mm (Table 1). Since the albedo and thermal conductivity are derived from the physical properties of black calcium carbonate shells and fully hydrated animal tissue respectively, they are unlikely to vary spatially or temporally. Because the mussel *M. californianus* frequently forms beds at least 8 cm deep, the mussel layer was considered to be 8 cm thick. The roughness height (z_0) of 8 mm was calculated as 0.1× mussel height, a standard meteorological approximation (Hansen, 1993).

(3) The mussel layers and the top rock layer were flooded with water at high tide, at a temperature of sea surface temperature (SST).

Mussel simulations used 20 layers over a total depth of 133 cm; there were 8 1-cm thick mussel layers, 2 1-cm thick rock layers, followed by rock layers of thickness 3 cm, 5 cm, 15 cm, and 5 rock layers of 20 cm thickness. The NOAH LSM allows a maximum of 20 soil layers. The distribution of thicknesses was chosen to provide at least 8 layers within the mussel bed itself, where the steepest temperature gradients occur. The deepest rock layer depth was chosen so that its temperature changed only seasonally. Output data were saved at 30 min intervals. Preserving the architecture of the NOAH LSM (Mitchell, 2005), parameter changes were made via configuration files, so that the model did not need to be re-compiled. In the future, the flexibility to make parameter changes via configuration files will make it possible to easily switch among organisms and substratum types for a range of ecological studies.

2.4. Model intercomparison

In order to evaluate model performance, we compared the NOAH Mussel Model results to results from both the NOAH LSM and the Gilman et al. (2006) model which is a representative one-of-a-kind model of mussel beds. The NOAH LSM includes neither the biophysical properties (e.g. thermal conductivity, specific heat) of mussel beds, nor the influence of ocean immersion. In our model intercomparison tests with the NOAH LSM, we used a black unvegetated soil with an albedo of 0.1, the same as used for the NOAH Mussel Model. Emissivity and roughness height are not adjustable in the NOAH LSM, so the long wave emissivity and roughness height were not identical to those used in the NOAH Mussel Model (Table 1). The NOAH LSM had permeable soil throughout, whereas the NOAH Mussel Model had impermeable granite rock layers. We expected extreme deviations of the NOAH LSM from observations when the data loggers were submerged at high tide because it lacked the influence of the ocean component.

The Gilman et al. (2006) model is a 1-dimensional model of heat transport through 50 1-cm layers representing 8 cm of mussels and 42 cm of underlying rock, with periodic submersion by the tide. The surface emissivity was 0.75, compared to 0.8 in the NOAH Mussel Model (Table 1). Surface albedo, roughness height, thermal conductivity and specific heat were the same as the NOAH Mussel Model (Table 1). This model made a simple linear approximation to surface evaporation and did not include passive convection (Table 1). This model will be referred to as the Gilman Model.

To assess the three models (NOAH Mussel Model, NOAH LSM, and Gilman Model), all three models were forced with identical environmental data as described in Section 2.5, and daily temperature trajectories from the models were compared to observational data from mussel biomimics as described in Section 3.1. The NOAH Mussel Model and the Gilman Model both include the biophysical properties of mussel beds and submersion by the tides. We therefore expected closer agreement between these models and observations than between the NOAH LSM and observations. Because the NOAH Mussel Model has a more complete description of the physics of evaporation, convection and interstitial water flow than the Gilman Model, we expected it to have the best agreement with observations.

2.5. Forcing data

As input, we used weather data from six sites (Tatoosh Island, Washington (48.39°N, 124.74°W), Boiler Bay, Oregon (44.83°N, 124.05°W), Pacific Grove, California (36.62°N, 121.90°W), Piedras Blancas, California (35.66°N, 121.28°W), Lompoc, California (34.72°N, 120.61°W), Alegria, California (34.47°N, 120.28°W)) over the period January 2000 to December 2004. Nine weather variables (air temperature, wind speed, relative humidity, air pressure, downwelling long- and short-wave radiation, precipitation rate, sea surface temperature, ocean water height) were linearly interpolated to 30 min intervals over the five-year period.

At each geographic location, we used meteorological data (air and sea surface temperature, wind speed, relative humidity, and precipitation rate) from the nearest station available in the National Climatic Data Center and National Data Buoy Center archives, and short-wave solar radiation and cloud cover from the University of Maryland Global Energy and Water Cycle Experiment (GEWEX) archive (Pinker et al., 2003; see Gilman et al., 2006 for details). Air pressure was estimated at a fixed value of 1013 h Pa, which is mean value of air pressure at sea level (Monteith and Unsworth, 1990). Long wave radiation was derived from air temperature, relative humidity, and cloud cover (TVA, 1972; Idso, 1981) for easier comparison with Gilman et al. (2006) who calculated long wave radiation in this way as part of their model runs. Ocean height was estimated from a combination of water level, which was simulated

by the Xtide tide prediction software (Flater, 2010), and wave run-up, which was calculated from offshore wave heights provided by the National Data Buoy Center by using a regression method (Harley and Helmuth, 2003). These same forcing data were used for all three models (NOAH LSM, NOAH Mussel Model, Gilman Model). The models were run without a spin-up period because the daily submersion by the tide in the NOAH Mussel Model and Gilman Model causes them to reach stability within 1–2 days.

3. Model validation

3.1. Observational data

Biomimetic data loggers (biomimics) were deployed in the center of the mussel bed at each of the sites (Fitzhenry et al., 2004). Each biomimic consisted of a Tidbit temperature logger (Onset Computer Corporation, Bourne, MA) embedded in polyester resin of similar size, shape, and color to *M. californianus*. There were usually three or more biomimics per site; numbers varied because of instrument loss due to storms. Topography in the rocky intertidal ecosystem is highly variable and microsites often have very large differences in temperature as a result of differences in slope and orientation (Helmuth and Hofmann, 2001; Seabra et al., 2011; Wethey, 2002). Biomimics were therefore placed in horizontal microsites in an attempt to standardize for the effects of topography. Previous comparisons of biomimics against living mussels have shown that these instruments record temperatures within approximately 2 °C of living mussels (Fitzhenry et al., 2004).

3.2. Statistics

We calculated error statistics for the deviations between model and observations, and among observations at each of the locations on the US west coast where we had *in situ* observations. We used the mean error (ME) and root mean square error (RMSE) as measures of deviation of the model results from the mean of the *in situ* biomimetic data logger observations. The ME measured whether the model trended overall warmer or cooler than observations. The RMSE is a conservative measure of the absolute magnitude of error and was used to determine model precision. Linear regression analyses were used to determine the overall fit between model results and observations. All calculations were carried out in the R statistical language.

The rocky intertidal ecosystem is a highly variable environment, and biomimics concurrently deployed in different microsites recorded different temperatures from one another due to differences in topography and wave splash (2.19 ± 1.62 °C mean ± SD, Fitzhenry et al., 2004). It is thus important to consider the amount of variability among the replicate observations at a site when assessing a model because the deviation between the model and the mean of the observational data may fall within the range of variation of the observational data. In order to account for environmental heterogeneity, we calculated the RMSE between the biomimic mean and each of the individual biomimics. Then the mean-individual RMSE were averaged for all the individual biomimics at a site. We compared the maximum of the RMSE among biomimics to the RMSE for the NOAH Mussel Model. This allowed us to determine whether the model predictions were within the range of environmental variance of empirically measured temperature within a sampling site. To estimate strength of the association between the mean of the logger observations and the model predictions, we undertook a linear regression analysis between the two, and reported the slope, intercept, their standard errors, and the R^2 for the regressions.

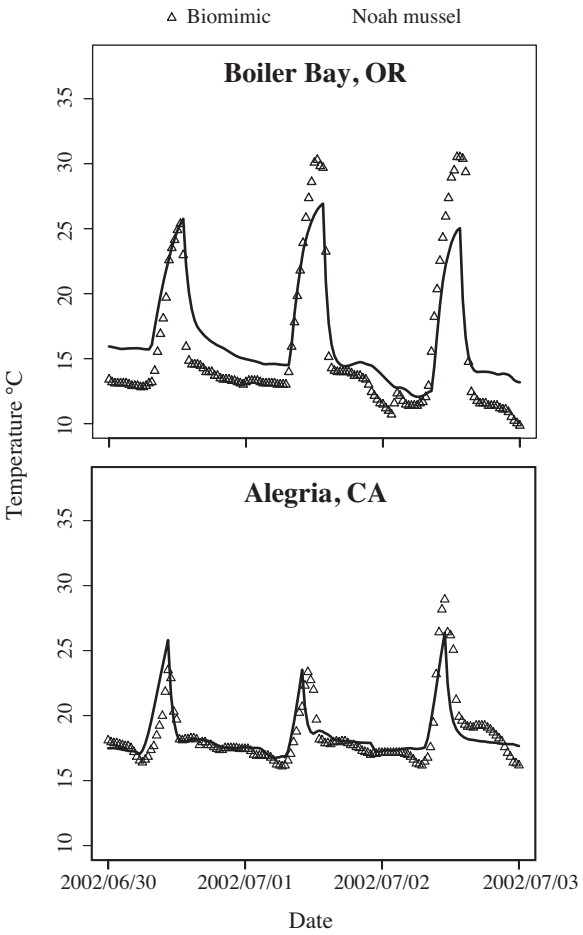

Fig. 2. Geographic comparison of daily observations and predictions. Values are means of biomimic observations (triangles) and NOAH Mussel Model predictions (lines) of intertidal temperatures (°C) at Boiler Bay, Oregon (top), and Alegria, California (bottom).

4. Model results

Fig. 2 compares the NOAH Mussel Model temperatures to the trajectories of mean biomimic temperature over a three day period at two latitudinally separated sites, Alegria, California (34.47°N) and Boiler Bay, Oregon (44.83°N). On a day to day basis there was general agreement in the temperature trajectories for the NOAH Mussel Model and the mean biomimic temperature (Fig. 2). Temperature deviations between observations and model at high tide are the result of differences between the forcing data (offshore sea surface temperatures measured by buoys) and onshore sea surface temperatures recorded by the biomimic loggers.

For the validation statistics, we only considered temperatures from the low tide (terrestrial) phase because both the ocean height and sea surface temperature were part of the common forcing dataset and thus high tide results were identical for the NOAH Mussel and Gilman Models. Table 2 shows the ME and RMSE of the model temperature trajectories as compared to the mean biomimic temperature trajectories. For all of the low tide (atmospheric condition) NOAH Mussel Model temperatures, five of the six sites had ME values that were within 1 °C of the mean biomimic temperature, and the sixth site had an ME value of 1.19 °C. At Lompoc, one of the two southernmost sites, the ME indicates that model temperatures during low tide trajectories were on average <0.1 °C lower than the mean biomimic temperature trajectories, whereas at the other southern sites, ME indicates that model temperatures during low tide trajectories were <1 °C higher than the mean biomimic

Table 2
Error statistics of the models relative to the mean biomimic temperature trajectories (ME = mean error, RMSE = root mean square error, n = number of observations). Upper panel: temperature trajectories during low tide, lower panel: daily maximum temperatures.

	Low tide (atmospheric conditions)						
	NOAH Mussel		NOAH LSM		Gilman Model		n
	ME	RMSE	ME	RMSE	ME	RMSE	
Tatoosh Island	1.19	2.31	0.87	7.27	1.30	2.61	5542
Boiler Bay	0.54	3.21	−1.81	7.33	0.55	3.44	6112
Pacific Grove	0.71	2.60	0.28	5.82	0.84	2.94	25,445
Piedras Blancas	0.82	2.92	2.36	11.33	0.82	3.39	12,191
Lompoc	−0.06	2.47	−1.18	5.60	−0.09	2.94	7415
Alegria	0.42	3.97	−0.64	4.40	0.68	4.43	5299
	Daily maximum						
	NOAH Mussel		NOAH LSM		Gilman Model		n
	ME	RMSE	ME	RMSE	ME	RMSE	
Tatoosh Island	−0.05	2.43	5.39	10.68	−0.20	2.79	285
Boiler Bay	−1.69	4.26	1.76	10.86	−2.06	4.49	429
Pacific Grove	−0.13	3.11	5.13	8.07	−0.29	3.31	1344
Piedras Blancas	−1.34	3.81	7.06	10.08	−1.85	4.01	1015
Lompoc	−2.14	4.50	5.84	8.94	−2.68	4.84	654
Alegria	−3.03	5.13	4.58	8.72	−3.16	5.25	458

temperature trajectories (Table 2). The NOAH LSM, which was run without ocean input or mussel thermal characteristics other than albedo, emissivity and roughness height, had low tide (atmospheric conditions) ME values closer to zero than the NOAH Mussel Model at two of the sites, Tatoosh and Pacific Grove (Table 2). This result for ME of the NOAH LSM is likely due to seasonal errors that cancel one another: too cold in winter and too warm in summer when the timing of low tide (and biomimic emergence) did not coincide with the coldest and hottest periods of the day (Fig. 3). The NOAH Mussel Model had low tide (terrestrial) phase ME values up to 0.21 °C closer to zero and daily maximum ME values 0.15–0.54 °C closer to zero than the Gilman Model at all of the sites (Table 2). The NOAH

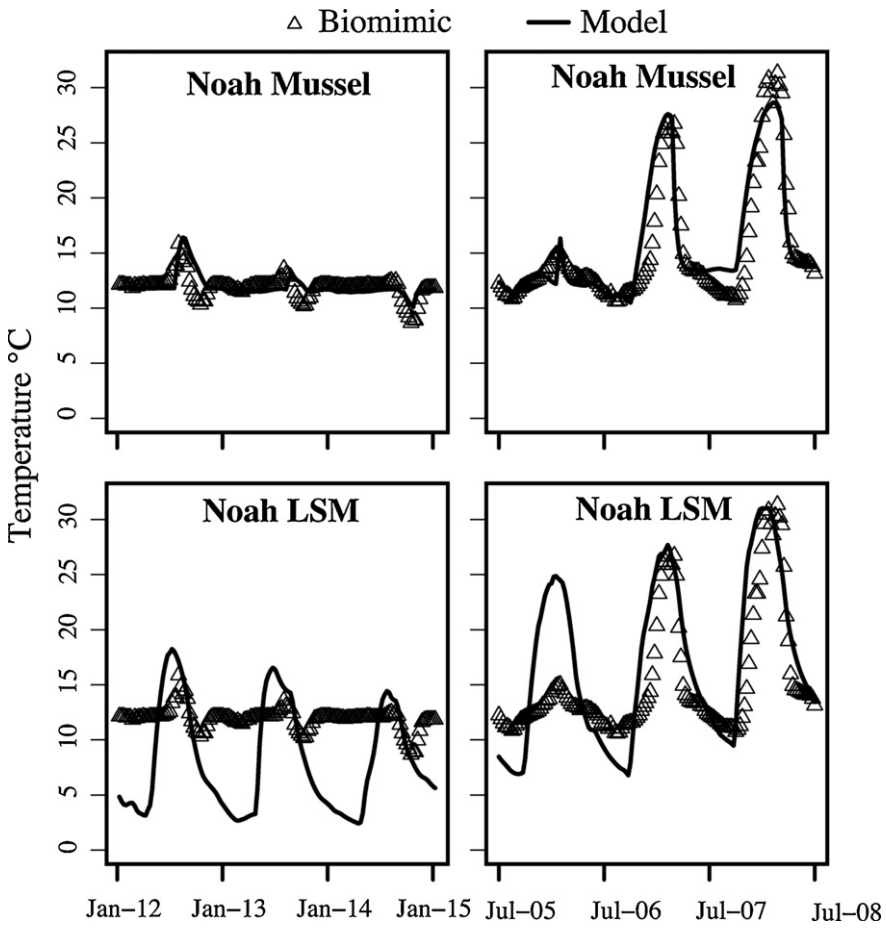

Fig. 3. Seasonal comparison of observations and predictions at Pacific Grove, California. Values are means of biomimic observations (triangles) and predictions (lines) of the NOAH Mussel Model and of the NOAH terrestrial model in winter (January) and summer (July).

Table 3
Correlation statistics of model trajectories versus biomimetic data logger trajectories.

	Tatoosh Island			
	R^2	Intercept ± error	Slope ± error	*df*
NOAH Mussel	0.751	−1.56 ± 0.11	1.03 ± 0.008	5540
NOAH LSM	0.049	10.51 ± 0.11	0.13 ± 0.007	5540
Gilman Model	0.673	−1.43 ± 0.13	1.01 ± 0.009	5540
	Boiler Bay			
	R^2	Intercept ± error	Slope ± error	*df*
NOAH Mussel	0.705	−2.79 ± 0.14	1.16 ± 0.010	6110
NOAH LSM	0.144	9.62 ± 0.13	0.31 ± 0.010	6110
Gilman Model	0.672	−3.99 ± 0.16	1.25 ± 0.011	6110
	Pacific Grove			
	R^2	Intercept ± error	Slope ± error	*df*
NOAH Mussel	0.699	1.99 ± 0.05	0.82 ± 0.003	25,443
NOAH LSM	0.390	9.21 ± 0.05	0.36 ± 0.003	25,443
Gilman Model	0.612	2.21 ± 0.06	0.80 ± 0.004	25,443
	Piedras Blancas			
	R^2	Intercept ± error	Slope ± error	*df*
NOAH Mussel	0.686	−0.60 ± 0.10	0.99 ± 0.006	12,189
NOAH LSM	0.008	15.47 ± 0.09	−0.05 ± 0.005	12,189
Gilman Model	0.566	−0.99 ± 0.13	1.01 ± 0.008	12,189
	Lompoc			
	R^2	Intercept ± error	Slope ± error	*df*
NOAH Mussel	0.715	0.24 ± 0.11	0.99 ± 0.007	7413
NOAH LSM	0.467	9.09 ± 0.08	0.42 ± 0.005	7413
Gilman Model	0.596	−0.66 ± 0.15	1.05 ± 0.010	7413
	Alegria			
	R^2	Intercept ± error	Slope ± error	*df*
NOAH Mussel	0.572	−5.02 ± 0.27	1.27 ± 0.015	5297
NOAH LSM	0.558	5.60 ± 0.15	0.69 ± 0.008	5297
Gilman Model	0.457	−4.58 ± 0.33	1.22 ± 0.018	5297

Mussel Model and Gilman Model had temperatures that were much closer to field measurements than the NOAH LSM (∼1 °C for average low tide error and up to 5 °C for daily maximum errors). Overall, the NOAH Mussel Model underestimated daily maximum mussel temperature by 2–3 °C in the south and by 0.1–1.7 °C in the north (Table 2). This result is similar to Ek et al. (2003) who observed that the NOAH LSM underestimated maximum air temperature at 2 m by 1–4 °C.

The NOAH Mussel Model had the smallest low tide (terrestrial) RMSE at all six sites and the smallest daily max RMSE at all six sites (Table 2). As predicted in Section 2.4, errors in the Gilman Model were comparable, but slightly higher, than those exhibited by the NOAH Mussel Model (Table 2). The low tide RMSE in the NOAH Mussel Model were less than 3 °C at four of the six sites (Table 2), which is better performance than that observed in terrestrial NOAH LSM simulations where RMSE are typically between 3 and 4 °C (Hong et al., 2009; Rosero et al., 2009). Table 3 shows the regression statistics for all of the models versus biomimic observations. The NOAH Mussel Model had the highest R^2 values of the three models, slightly higher than the Gilman Model and markedly higher than the NOAH LSM. Ideal regressions of model predictions versus observations have a *y*-intercept of zero and a slope of one. The NOAH Mussel Model and the Gilman Model were closer to the ideal result for all sites than the NOAH LSM, and had similar *y*-intercepts and slopes (Table 3). At all sites, the biomimetic sensor observations and NOAH Mussel Model predictions were well correlated during the low tide (terrestrial) phase (Fig. 4).

Table 4 compares the biomimic temperatures from individual microsites with the mean biomimic temperatures to determine whether model predictions were within the range of among-microsite variability. Typically, there was more variability, lower R^2, and higher RMSE at the lower latitude sites compared to the higher latitude sites. By comparing the RMSE of the observational data with NOAH Mussel Model RMSE, we found that the model RMSE was no more than 1.38 °C larger than the largest microsite RMSE (Table 4). At Lompoc the model RMSE was 1.95 °C less than the largest microsite RMSE (Table 4).

5. Discussion

Measuring and predicting the impacts of global climate change, at a wide range of temporal and spatial scales, have emerged as research priorities that span disciplines (e.g. Hansen et al., 2006; Helmuth et al., 2006b; Lavergne et al., 2010; Parmesan, 2006; Wethey et al., 2011). Predicting patterns of weather and climate is complex; and while significant progress has been made at generating regional forecasts, predicting changes in weather and climate at smaller scales remains difficult. Despite the large spatial scale of weather and climate models, organisms actually experience only the microclimate of their local environment (Kearney and Porter, 2004). For an intertidal organism such as a mussel, this "world view" is thus on the order of centimeters to meters. Methods that bridge the gap from large-scale atmospheric-scale processes to

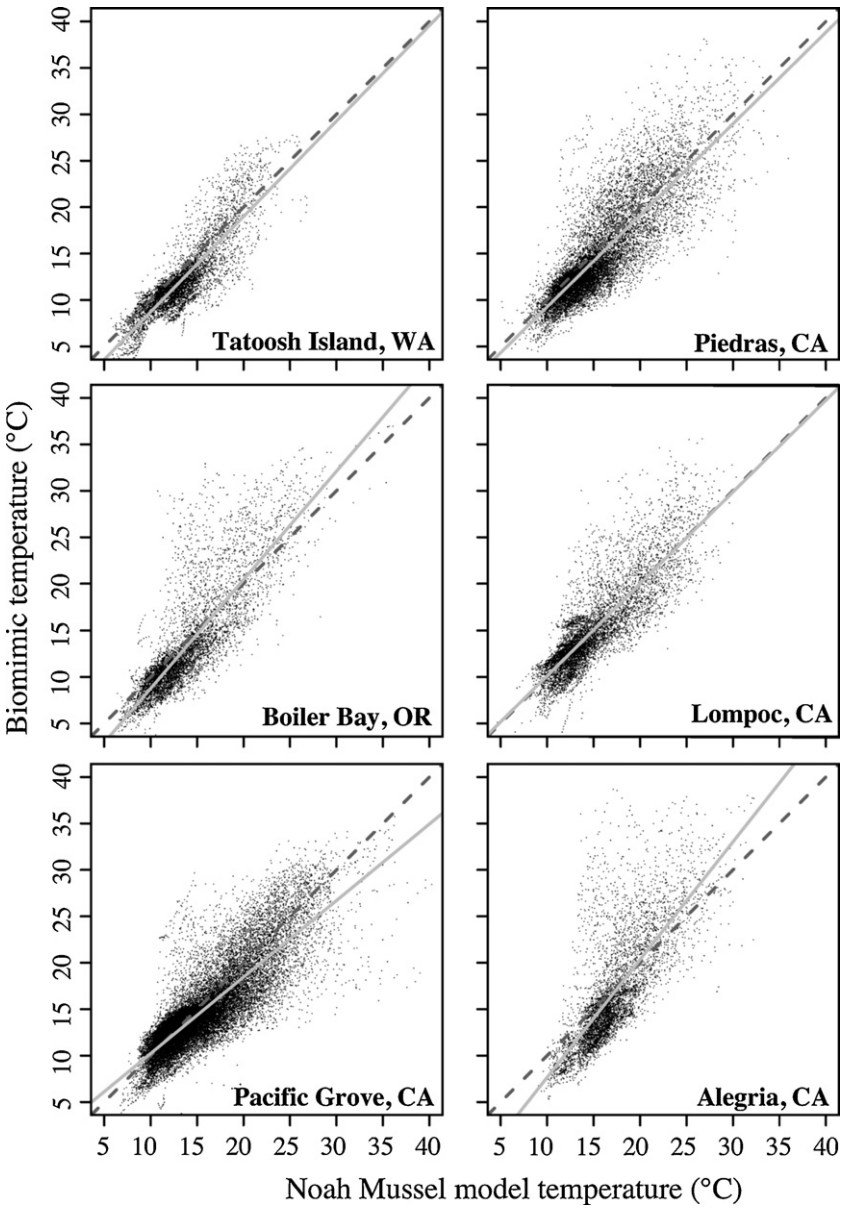

Fig. 4. Relation between NOAH Mussel Model predictions and mean biomimetic temperature observations. Dots are individual observations spaced by 30 min, solid lines are linear regressions, and dotted lines are 1:1 lines.

Table 4
Error statistics of NOAH Mussel Model compared to variability among biomimetic data loggers during low tide. Biomimic mean versus NOAH Mussel Model R^2 is the correlation statistic between the average of the data loggers and the model predictions at the same times of day. Among biomimic RMSE is the average deviation of the individual biomimetic data loggers from the logger average. Maximum biomimic RMSE is the RMSE from the logger that deviated the most from the logger mean. NOAH Mussel Model RMSE is the deviation of the model predictions at low tide from the logger means at the same times of day.

	Biomimic mean versus NOAH Mussel Model R^2 (mean ± SD)	Among biomimic RMSE (mean ± SD)	Maximum biomimic RMSE	NOAH Mussel Model RMSE
Tatoosh Island	0.951 ± 0.041	1.10 ± 0.44	1.73	2.31
Boiler Bay	0.941 ± 0.028	1.79 ± 0.14	2.00	3.21
Pacific Grove	0.904 ± 0.025	1.50 ± 0.22	1.79	2.60
Piedras Blancas	0.889 ± 0.033	1.55 ± 0.26	1.87	2.92
Lompoc	0.826 ± 0.061	2.82 ± 1.12	4.42	2.47
Alegria	0.896 ± 0.071	1.87 ± 0.49	2.59	3.97

those at the local scale of the organism are therefore vital if we are to model the ecological impacts of climate change.

Prior workers have used heat and mass budget models of individual organisms in order to model organism temperatures (e.g. Bell, 1995; Buckley, 2008; Gates, 1980; Helmuth, 1998; Kearney and Porter, 2004; Miller et al., 2009; Tracy, 1976). However, as this study demonstrates, it is possible to estimate organismal body temperatures of broadscale space-occupiers or bed-forming species by transforming land surface models, which calculate mass, heat, and momentum fluxes between the atmosphere and the ground. By

taking into account the effects of different kinds of soil, plant and animal cover for additional organisms, one can obtain comparable results to organism-specific heat budget models such as Gilman et al. (2006) (Tables 2–4). In models of the intertidal zone, the ocean component was particularly important, and was one of the primary reasons that the NOAH LSM produced high RMSE and low R^2 values when compared to biomimic observations (Tables 2 and 3, Fig. 3). Both the NOAH Mussel Model and the Gilman Model predicted mussel temperatures for the entire low tide (atmospheric conditions) phase better than for the daily maximum mussel temperatures (Table 2). This was expected because pinpointing a single point such as a daily maximum is a much more difficult task than determining overall trajectories. Table 2 shows that the NOAH Mussel Model RMSE for the daily maxima was <1.16 °C above the RMSE for the low tide phase for all the sites except for Lompoc, which we found to be acceptable considering the difficulties in determining this statistic. This low tide RMSE is lower than the typical midday surface temperature RMSE values of 3–4 °C observed with the NOAH LSM in the North American Land Data Assimilation System (Mitchell et al., 2004), indicating that the NOAH Mussel Model performs well compared to its terrestrial counterpart. The ability to determine daily maxima using models such as the NOAH Mussel Model will be critical for predicting the impacts of future climate change on intertidal communities because this measure can be used to determine when mussel physiological tolerance thresholds are exceeded.

Biomimic observations of mussel temperatures were essential for verifying these models, but have their own sources of variability. In general, the intertidal environment is subject to extreme temperature heterogeneity due to variations in small-scale topography and timing of submergence (Wethey, 2002; Denny et al., 2011), and even though replicate biomimics were placed in seemingly similar microhabitats, there were still average deviations in the replicate observations among biomimics ranging from 1.10 to 2.64 °C, with maximum microsite deviations ranging from 1.87 to 4.42 °C (Table 4). Also, biomimics were occasionally overgrown by barnacles and surrounding mussels, which may have impacted their observations relative to other replicates. The largest observation-based microsite RMSE values were between 63 and 75% of the magnitude of the model RMSE at all sites except Lompoc (Table 4), indicating that microsite variation accounts for 63–75% of model RMSE. Among-biomimic RMSE was particularly high in Lompoc and the largest observation-based microsite RMSE was180% of model RMSE (Table 4). This high microsite variability at Lompoc may explain the difference in the NOAH Mussel Model RMSE for the low tide (atmospheric conditions) phase versus the daily maximum (Table 2).

Because we treated large-scale space occupiers as "vegetation" layers, the model is easily modified to simulate other kinds of organisms like barnacles, by changing readily measurable parameters such as surface albedo, biological layer thickness, and surface roughness scale (Jones et al., personal communication). The model has also been used to simulate heat transport in intertidal sand flats, by using unvegetated sand layers instead of rocky substrata (Woodin et al., 2010). The model architecture allows these modifications to be made at run-time via configuration files, so that the model does not need to be re-compiled in order to change among substrata or organisms (Mitchell, 2005). By taking into account the 3D geometry of solar radiation on surfaces of arbitrary slope and orientation (e.g. Gates, 1980; Miller et al., 2009; Wethey, 2002), land surface models can also be used in topographically complex environments.

The ability to predict the body temperatures of a broad range of intertidal species is essential for our understanding the mechanisms responsible for biological responses to climate change. Intertidal ecosystems are likely to be particularly sensitive to changes in climate because many intertidal organisms live close to their tolerance limits (Foster, 1969; Somero, 2002; Southward, 1958). Land surface models, as shown here, can be used retrospectively to assess the impact of climate and climate change on patterns of distribution and abundance, as well as their effects on biogeography on local and continental spatial scales, and on multi-decadal time scales (e.g. Gilman et al., 2006; Wethey, 2002; Wethey and Woodin, 2008). They can also be used in both short- and long-term forecasting of thermal stress in the intertidal zone (Mislan and Wethey, 2011). Organism temperature is important ecologically because differences in responses to temperature can alter the dynamics of competition and predation, leading to cascading effects on the rest of an ecosystem (Pincebourde et al., 2008; Poloczanska et al., 2008; Wethey, 2002). Because coastal habitats are often comprised of "mosaics" rather than smooth gradients in thermal stress (Fischer-Piette, 1955; Helmuth et al., 2006a; Mislan et al., 2009; Berke et al., 2010), tools such as the land surface models described here are essential for understanding biogeographic patterns of physiological stress and mortality risk.

Author contributions

Wethey conceived the idea and oversaw the modification and testing of the NOAH Mussel Model. Brin did the software modifications and testing of the model. Mislan did the model intercomparison simulations and statistical analyses. Helmuth collected the validation data and designed the biomimetic loggers. Wethey and Mislan led the writing.

Acknowledgments

Supported by grants from NSF (OCE0323364, OCE0926581 and OCE1039513), NOAA (NA04NOS4780264), NASA (NNG04GE43G and NNX07AF20G), and a NASA Earth Systems Science Fellowship. We thank Sarah Gilman for assembling the weather data. Sarah Woodin and two anonymous reviewers made very helpful suggestions for improving the manuscript.

References

Bayne, B.L., Bayne, C.J., Carefoot, T.C., Thompson, R.J., 1976. Physiological ecology of *Mytilus californianus* Conrad. 1. Metabolism and energy balance. Oecologia 22, 211–228.

Bayne, B.L., Worrall, C.M., 1980. Growth and production of mussels, *Mytilus edulis* from two populations. Mar. Ecol. Progr. Ser. 3, 317–328.

Bell, E.C., 1995. Environmental and morphological influences on thallus temperature and desiccation of the intertidal alga *Mastocarpus papillatus* Kützing. J. Exp. Mar. Biol. Ecol. 191, 29–55.

Beniston, M., Stephenson, D.B., Christensen, O.B., et al., 2007. Future extreme events in European climate: an exploration of regional climate model projections. Clim. Change 81, 71–95.

Berke, S.K., Mahon, A.R., Lima, F.P., Halanych, K.M., Wethey, D.S., Woodin, S.A., 2010. Range shifts and species diversity in marine ecosystem engineers: patterns and predictions for European sedimentary habitats. Global Ecol. Biogeogr. 19, 223–232.

Buckley, L.B., 2008. Linking traits to energetics and population dynamics to predict lizard ranges in changing environments. Am. Nat. 171, E1–E19.

Chen, F., Dudhia, J., 2001. Coupling an advanced land surface-hydrology model with the Penn State-NCAR MM5 modeling system. Month Weath. Rev. 129, 569–585.

Christensen, J.H., Hewitson, B., Busuioc, A., Chen, A., Gao, X., et al., 2007. Regional climate projections. In: Solomon, S., Qin, D., Manning, M., Chen, Z., et al. (Eds.), Climate Change 2007: The Physical Science Basis. Contribution of Working Group 1 to the Fourth Assessment Report of the Intergovernmental Panel on Climate Change. Cambridge, UK, Cambridge University Press, pp. 849–940.

Connell, J.H., 1961. The influence of interspecific competition and other factors on the distribution of the barnacle *Chthamalus stellatus*. Ecology 42, 710–723.

Denny, M.W., Dowd, W.W., Bilir, L., Mach, K.J., 2011. Spreading the risk: small-scale body temperature variation among intertidal organisms and its implications for species persistence. J. Exp. Mar. Biol. Ecol. 400, 175–190.

Ek, M.B., Mitchell, K.E., Lin, Y., Rogers, E., Grunmann, P., Koren, V., et al., 2003. Implementation of NOAH land surface model advances in the National Centers for Environmental Prediction operational mesoscale Eta model. J. Geophys. Res. 108, D22, 8851, doi:10.1029/2002JD003296.

Finke, G.R., Bosinovic, F., Navarrete, S.A., 2009. A mechanistic model to study the thermal ecology of a southeastern Pacific dominant intertidal mussel and implications for climate change. Physiol. Biochem. Zool. 82, 303–313.
Fischer-Piette, E., 1955. Répartition, le long des côtes septentrionales de l'espagne, des principales espèces peuplant les rochers intercotidaux. Ann. Inst. Océanogr. Monaco 31, 37–124.
Fitzhenry, T., Halpin, P.M., Helmuth, B., 2004. Testing the effects of wave exposure, site, and behavior on intertidal mussel body temperatures: applications and limits of temperature logger design. Mar. Biol. 145, 339–349.
Flater, D., 2010. Xtide, Online document: http://www.flaterco.com/xtide (accessed 30.1.11).
Foster, B.A., 1969. Tolerance of high temperatures by some intertidal barnacles. Mar. Biol. 4, 326–332.
Foster, B.A., 1971. Desiccation as a factor in the intertidal zonation of barnacles. Mar. Biol. 8, 12–29.
Gates, D.M., 1980. Biophysical Ecology. Springer, New York.
Gilman, S.E., Wethey, D.S., Helmuth, B., 2006. Variation in the sensitivity of organismal body temperature to climate change over local and geographic scales. Proc. Natl. Acad. Sci. U.S.A. 103, 9560–9565.
Hansen, J., Saton, M., Ruedy, R., Lo, K., Lea, D.W., Medina-Elizade, M., 2006. Global temperature change. Proc. Natl. Acad. Sci. U.S.A. 103, 14288–14293.
Hansen, F.V., 1993. Surface Roughness Lengths. Report ARL-TR-61. Army Research Laboratory.
Harley, C.D.G., Helmuth, B.S.T., 2003. Local and regional scale effects of wave exposure, thermal stress and absolute vs. effective shore level on patterns of intertidal zonation. Limnol. Oceanogr. 48, 1498–1508.
Helmuth, B.S.T., 1998. Intertidal mussel microclimates: predicting the body temperature of a sessile invertebrate. Ecol. Monogr. 68, 51–74.
Helmuth, B., Broitman, B.R., Blanchette, C.A., et al., 2006a. Mosaic patterns of thermal stress in the rocky intertidal zone: implications for climate change. Ecol. Monogr. 76, 461–479.
Helmuth, B.S.T., Hofmann, G.E., 2001. Microhabitats, thermal heterogeneity, and patterns of physiological stress in the rocky intertidal zone. Biol. Bull. 201, 374–384.
Helmuth, B., Mieszkowska, N., Moore, P., Hawkins, S.J., 2006b. Living on the edge of two worlds: forecasting the responses of rocky intertidal ecosystems to climate change. Annu. Rev. Ecol. Evol. Syst. 37, 373–404.
Hong, S., Lakshmi, V., Small, E.E., Chen, F., Tewari, M., Manning, K.W., 2009. Effects of vegetation and soil moisture on the simulated landsurface processes from the coupled WRF/NOAH model. J. Geophys. Res. 114, D18118, doi:10.1029/2009JD011249.
Idso, S.B., 1981. A set of equations for full spectrum 8- to 14-μm and 10.5 to 12.5-μm thermal radiation from cloudless skies. Water Resour. Res. 17, 295–304.
Jones, S.J., Mieszkowska, N., Wethey, D.S., 2009. Linking thermal tolerances and biogeography: *Mytilus edulis* (L.) at its southern limit on the east coast of the United States. Biol. Bull. 217, 73–85.
Jones, S.J., Lima, F.P., Wethey, D.S., 2010. Rising environmental temperatures and biogeography: poleward range contraction of the blue mussel, *Mytilus edulis* L., in the western Atlantic. J. Biogeogr. 37, 2243–2259.
Kearney, M., Porter, W.P., 2004. Mapping the fundamental niche: physiology, climate, and the distribution of a noctural lizard. Ecology 85, 3119–3131.
Lavergne, S., Mouquet, N., Thuiller, W., Ronce, O., 2010. Biodiversity and climate change: integrating evolutionary and ecological responses of species and communities. Annu. Rev. Ecol. Evol. Syst. 41, 321–350.
Lewis, J.R., 1964. The Ecology of Rocky Shores. English Universities Press, London.
Mesinger, F., DiMego, G., Kalnay, E., Mitchell, K., Shafran, P.C., Ebisuzaki, W., et al., 2006. North American regional reanalysis. Bull. Am. Meteorol. Soc. 87, 343–360.
Miller, L.P., Harley, C.D.G., Denny, M.W., 2009. The role of temperature and desiccation stress in limiting the local-scale distribution of the owl limpet, *Lottia gigantea*. Funct. Ecol. 23, 756–767.
Mislan, K.A.S., Wethey, D.S., Helmuth, B., 2009. When to worry about the weather: role of tidal cycle in determining patterns of risk in intertidal ecosystems. Global Change Biol. 15, 3056–3065.
Mislan, K.A.S., Wethey, D.S., 2011. Gridded meteorological data as a resource for mechanistic macroecology in coastal environments. Ecol. Appl., doi:10.1890/10-2049.1.
Mitchell, K., 2005. Noah LSM User Guide 2.7.1. NOAA Environmental Modeling Center, Camp Springs, MD, Online document http://www.emc.ncep.noaa.gov/mmb/gcp/noahlsm/Noah_LSM_USERGUIDE_2.7.1.htm (accessed 2.8.11).
Mitchell, K.E., Lohmann, D., Houser, P.R., Wood, E.F., Schaake, J.C., Robock, A., et al., 2004. The multi-institution North American Land Data Assimilation System (NLDAS): utilizing multiple GCIP products and partners in a continental distributed hydrological modeling system. J. Geophys. Res. 109, D07S90, doi:10.1029/2003/JD003823.
Monteith, J.L., Unsworth, M.H., 1990. Principles of Environmental Physics. Edward Arnold, London, UK.
Morris, R.H., Abbott, D.P., Haderlie, E.C., 1980. Intertidal Invertebrates of California. Stanford University Press, Palo Alto, CA.
Paine, R.T., 1966. Food web complexity and species diversity. Am. Nat. 100, 65–75.
Paine, R.T., 1974. Intertidal community structure: experimental studies on the relationship between a dominant competitor and its principal predator. Oecologia 15, 93–120.
Pinker, R.T., Tarpley, J.D., Laszlo, I., Mitchell, K.E., Houser, P.R., et al., 2003. Surface radiation budgets in support of the GEWEX continental-scale international project (GCIP) and the GEWEX Americas prediction project (GAPP), including the North American land data assimilation system (NLDAS) project. J. Geophys. Res. 108, D22, 8844.
Parmesan, C., 2006. Ecological and evolutionary responses to recent climate change. Annu. Rev. Ecol. Evol. Syst. 37, 637–669.
Pincebourde, S., Sanford, E., Helmuth, B., 2008. Body temperature during low tide alters the feeding performance of a top intertidal predator. Limnol. Oceanogr. 43, 1562–1573.
Poloczanska, E.S., Hawkins, S.J., Southward, A.J., Burrows, M.T., 2008. Modeling the response of competing species to climate change. Ecology 89, 3138–3149.
Rosero, E., Yang, Z-L., Gulden, L.E., Niu, G-Y., 2009. Evaluating enhanced hydrological representations in NOAH LSM over transition zones: implications for model development. J. Hydrometeorol. 10, 600–622.
Saha, S., Moorthi, S., Pan, H-L., Wu, X., Wang, J., Nadiga, S., et al., 2010. The NCEP climate forecast system reanalysis. Bull. Am. Meteorol. Soc. 91, 1015–1057.
Seabra, R., Wethey, D.S., Santos, A.M., Lima, F.P., 2011. Side matters: microhabitat influence on intertidal heat stress over a large geographical scale. J. Exp. Mar. Biol. Ecol. 400, 200–208.
Somero, G.N., 2002. Thermal physiology and vertical zonation of intertidal animals: optima, limits, and costs of living. Integr. Comp. Biol. 42, 780–789.
Southward, A.J., 1958. Note on the temperature tolerances of some intertidal animals in relation to environmental temperatures and geographical distribution. J. Mar. Biol. Assoc. UK 37, 49–66.
Szathmary, P.L., Helmuth, B., Wethey, D.S., 2009. Climate change in the rocky intertidal zone: predicting and measuring the body temperature of a keystone predator. Mar. Ecol. Progr. Ser. 374, 43–56.
Tennesee Valley Authority, 1972. Heat and Mass Transfer between a Water Surface and the Atmosphere. Water Resources Laboratory Report 14. TVA Engineering Lab, Norris, Tenn.
Tracy, C.R., 1976. A model of the dynamic exchanges of water and energy between a terrestrial amphibian and its environment. Ecol. Monogr. 46, 293–326.
Wethey, D.S., 2002. Microclimate, competition, and biogeography: the barnacle *Chthamalus fragilis* in New England. Integr. Comp. Biol. 42, 872–880.
Wethey, D.S., Woodin, S.A., 2008. Ecological hindcasting of biogeographic responses to climate change in the European intertidal zone. Hydrobiologia 606, 139–151.
Wethey, D.S., Woodin, S.A., Hilbish, T.J., Jones, S.J., Lima, F.P., Brannock, P.M., 2011. Response of intertidal populations to climate: effects of extreme events versus long term change. J. Exp. Mar. Biol. Ecol. 400, 132–144.
Widdows, J., Bayne, B.L., 1971. Temperature acclimation of *Mytilus edulis* with reference to its energy budget. J. Mar. Biol. Assoc. UK 51, 827–843.
Williams, G.A., De Pirro, M., Leung, K.M.Y., Morritt, D., 2005. Physiological responses to heat stress on a tropical shore: the benefits of mushrooming behaviour in the limpet *Cellana grata*. Mar. Ecol. Progr. Ser. 292, 213–224.
Wolcott, T.G., 1973. Physiological ecology and intertidal zonation in limpets (*Acmaea*): a critical look at limiting factors. Biol. Bull. 145, 389–422.
Woodin, S.A., Wethey, D.S., Volkenborn, N., 2010. Infaunal hydraulic ecosystem engineers: cast of characters and impacts. Integr. Comp. Biol. 50, 176–187.